

Immobilization of the Gas Signaling Molecule H₂S by Radioisotopes: Detection, Quantification, and In Vivo Imaging

Swarbhanu Sarkar⁺, Yeong Su Ha⁺, Nisarg Soni⁺, Gwang Il An⁺, Woonghee Lee, Min Hwan Kim, Phuong Tu Huynh, Heesu Ahn, Nikunj Bhatt, Yong Jin Lee, Jung Young Kim, Kwon Moo Park, Isao Ishii, Shin-Geol Kang, and Jeongsoo Yoo*

Abstract: Hydrogen sulfide (H₂S) has multifunctional roles as a gas signaling molecule in living systems. However, the efficient detection and imaging of H₂S in live animals is very challenging. Herein, we report the first radioisotope-based immobilization technique for the detection, quantification, and in vivo imaging of endogenous H₂S. Macrocyclic ⁶⁴Cu complexes that instantly reacted with gaseous H₂S to form insoluble ⁶⁴CuS in a highly sensitive and selective manner were prepared. The H₂S concentration in biological samples was measured by a thin-layer radiochromatography method. When ⁶⁴Cu-cyclen was injected into mice, an elevated H₂S concentration in the inflamed paw was clearly visualized and quantified by Cerenkov luminescence and positron emission tomography (PET) imaging. PET imaging was also able to pinpoint increased H₂S levels in a millimeter-sized infarcted lesion of the rat heart.

Hydrogen sulfide (H₂S) was the third gaseous signaling molecule to be identified, after NO and CO. H₂S is an important signaling mediator for a wide range of physiological and pathological functions.^[1] The level of endogenous H₂S is very low and is tightly regulated in living organisms. Alterations in H₂S levels are associated with many diseases, such as inflammation, hypertension, atherosclerosis, diabetes, Alzheimer's disease, and cancer.^[2] However, considering its importance in biology and medicine, research tools for the precise detection and quantification of H₂S are very limited.^[3] Specifically, the lack of a noninvasive imaging technique for

whole-body monitoring of H₂S is a major obstacle to efficient H₂S research in live animals, including humans.

There are several known hydrogen sulfide detection methods.^[4] However, because all of these methods were originally developed to measure H₂S in nonbiological samples, they are destructive and require harsh sample-preparation steps.^[5] Furthermore, the volatility of H₂S gas and its chemical complexity in biological systems (labile, bound, and free H₂S and polysulfides) make the precise detection of H₂S more challenging.^[4]

Imaging techniques based on fluorescent dyes have emerged as new detection methods for H₂S.^[6] The most widely utilized strategies to capture sulfide take advantage of its redox,^[7] demetalation,^[8] or nucleophilic properties.^[9] Even though these new approaches have several advantages, their applications in live-animal imaging are limited, mainly because of the low tissue penetration of emitted fluorescent light. The typical maximum tissue penetration for optical imaging is less than 1 cm.^[10] Only a few proof-of-concept imaging studies have been performed, on small worms,^[11] transparent zebra fish,^[12] and mice (at shallow skin depths).^[13] To detect endogenous H₂S inside animal bodies and potentially in humans without a detection-depth issue, the development of a new class of imaging probes is required.^[14] Herein, we report new radioactive probes for the efficient detection, accurate quantification, and nuclear imaging of H₂S in live animals.

H₂S reacts with copper(II) ions to form insoluble copper sulfide (CuS, solubility product $K_{sp} = 8.0 \times 10^{-36}$) in aqueous solutions^[15] (Figure 1a). We hypothesized that if we could trap volatile H₂S gas in a solid form by using radioactive copper ions, we could detect and quantify H₂S accurately on the basis of the high sensitivity of these radioisotopes. First, to identify a copper complex with appropriate stability, that is, one labile enough to react with hydrogen sulfide at high reactivity but robust enough against other competing biological components, we prepared 20 ⁶⁴Cu complexes by radiolabeling 20 carefully selected chelators (see Figure S1 in the Supporting Information). Of these 20, 12 were synthesized to study the effects of coordination atoms, substituents, steric hindrance, stereostructure, and cross-bridging (see the Supporting Information). Copper-64 has a half-life of 12.7 h and decays by positron emission (β^+ , 17.8 %), which enables high-quality positron emission tomography (PET) imaging. The radiolabeling step was completed by mixing ⁶⁴CuCl₂ (37–740 MBq) with the appropriate chelators (1–100 μ g) in ammonium acetate buffer (0.1 M, pH 6.8), by simple shaking for 5–20 min at 60 °C. Quantitative radiolabeling was con-

[*] Dr. S. Sarkar,^[+] Y. S. Ha,^[+] N. Soni,^[+] W. Lee, P. T. Huynh, H. Ahn, Dr. N. Bhatt, Prof. K. M. Park, Prof. J. Yoo
Department of Molecular Medicine, Department of Anatomy
BK21 Plus Program, Kyungpook National University
Daegu 41944 (Korea)
E-mail: yooj@knu.ac.kr

Dr. G. I. An,^[+] M. H. Kim, Dr. Y. J. Lee, Dr. J. Y. Kim
Molecular Imaging Research Centre
Korea Institute of Radiological and Medical Sciences
Seoul 01812 (Korea)

Prof. I. Ishii
Department of Biochemistry, Keio University
Tokyo 105-8512 (Japan)

Prof. S.-G. Kang
Department of Chemistry, Daegu University
Gyeongsan 38453 (Korea)

[+] These authors contributed equally.

Supporting information for this article can be found under:
<http://dx.doi.org/10.1002/anie.201603813>.

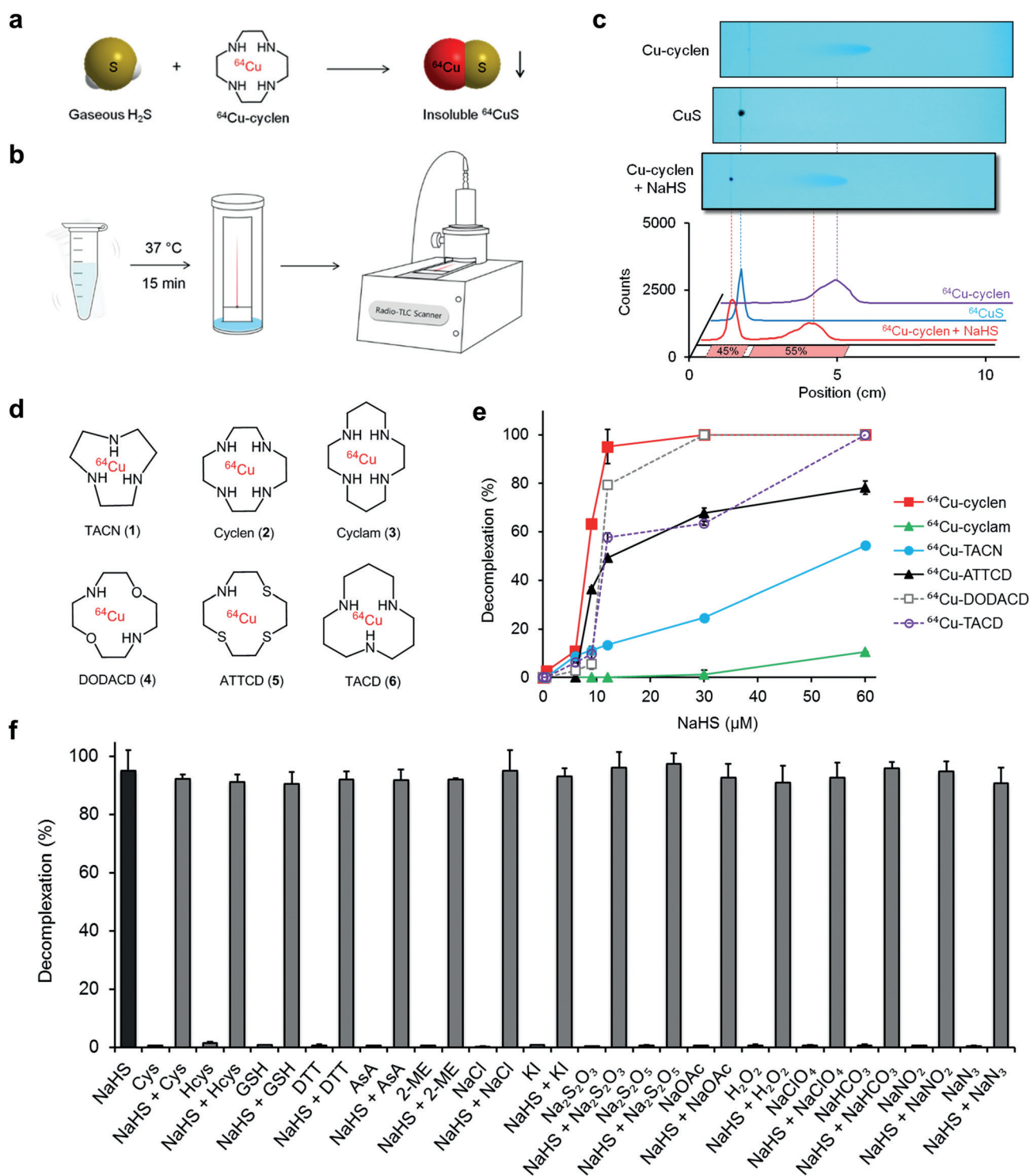


Figure 1. Radioactive copper complexes and their sensitivity and selectivity for H_2S . a) Decomplexation of ^{64}Cu -cyclen by H_2S . b) Schematic representation of H_2S detection by the radio-TLC method. c) TLC profiles of nonradioactive Cu-cyclen, CuS, and a reaction mixture of Cu-cyclen and H_2S , and their corresponding radio-TLC chromatograms. d) The six ^{64}Cu complexes screened. e) Sensitivity results of the six probes. f) Selectivity of ^{64}Cu -cyclen towards H_2S over various biological competitors.

firmed by thin-layer radiochromatography (radio-TLC). The radiolabeled complexes did not require additional purification for the following in vitro and in vivo experiments.

The radiolabeled Cu^{II} complexes were then tested for their sensitivity and selectivity for H_2S . Sufficiently labile

^{64}Cu -labeled complexes, such as ^{64}Cu -cyclen, were found to react with H_2S to form insoluble ^{64}CuS precipitates (Figure 1a). The resulting ^{64}CuS could be separated readily from the intact initial complex by thin-layer chromatography (TLC) and could also be accurately quantified by using

a radio-TLC scanner (Figure 1b). Whereas intact complexes move along with the developing solvent (methanol/10% ammonium acetate, 1:1), formed CuS remains at the spotting origin on the C18 TLC plate (Figure 1c, top). The retention values (R_f) of the radiolabeled complex matched with those of the nonradioactive copper complex. The decomplexation percentage was calculated from the integration ratio of the ^{64}Cu complex and ^{64}CuS peaks in the radio-TLC chromatograms (Figure 1c, bottom).

For the sensitivity test, we first assessed all radiolabeled complexes with a freshly prepared 60 μM sodium hydrosulfide (NaHS) solution. NaHS reaches equilibrium rapidly and essentially exists in both NaHS and H_2S forms in water.^[3] The mixture of the ^{64}Cu complex (ca. 1.85 MBq) and NaHS solution (500 μL) was shaken at 37°C for 15 min, vortexed, spotted on a TLC plate, developed, and analyzed with a radio-TLC scanner. Among the 20 tested complexes, nine complexes (probes **1**, **2**, **3**, **4**, **5**, **6**, **7**, **10**, **19**) showed some reactivity, that is, decomplexation and ^{64}CuS formation (see Table S1 in the Supporting Information). The remaining 11 complexes were highly intact at this concentration. Generally, non-substituted simple macrocyclic chelators showed higher reactivity with NaHS. The most promising six complexes, presenting different macrocyclic backbones (Figure 1d), were selected and tested at lower concentrations of NaHS. ^{64}Cu -cyclen (**2**) showed the highest sensitivity, followed by ^{64}Cu -DODACD (**4**) and ^{64}Cu -TACD (**6**), whereas ^{64}Cu -cyclam (**3**) showed the lowest sensitivity (Figure 1e). At a concentration of 12 μM NaHS, ^{64}Cu -cyclen showed nearly quantitative demetalation. The minimum detection limit of NaHS with ^{64}Cu -cyclen was calculated to be 0.15 μM (see Figure S2). Other azamacrocyclic complexes with a smaller or larger ring size (TACN, cyclam, TACD) showed less sensitivity for H_2S . Any replacement of the nitrogen atoms of cyclen with oxygen or sulfur (DODACD and ATTCD) also decreased the sensitivity. When the reactivity of the six ^{64}Cu complexes was tested with 60 μM NaHS, the fastest reactivity was observed with ^{64}Cu -TACD and ^{64}Cu -DODACD, followed by ^{64}Cu -cyclen. All three complexes showed 100% decomplexation within 5 min (see Figure S3).

We then tested the selectivity of six probes for H_2S in the presence of other potential competitors, such as biothiols, inorganic sulfur compounds, anions, and oxidants, under biological conditions (see Table S2). ^{64}Cu -cyclen showed practically no decomplexation in the presence of abundant biologically relevant thiols, such as glutathione (GSH, 10 mM), L-cysteine (Cys, 1 mM), and homocysteine (Hcys, 1 mM). ^{64}Cu -cyclen also showed high robustness in the presence of other thiols (2-mercaptoethanol (2-ME), DL-dithiothreitol (DTT)), inorganic sulfur compounds ($\text{S}_2\text{O}_3^{2-}$, $\text{S}_2\text{O}_5^{2-}$), reducing agents (ascorbic acid (AsA)), inorganic nucleophiles (Cl^- , I^- , OAc^- , ClO_4^- , HCO_3^- , NO_2^- , N_3^-), and reactive oxygen species (H_2O_2) at a minimum concentration of 100 μM . However, upon the addition of 12 μM NaHS, all reactions showed nearly quantitative decomplexation, regardless of the presence of competing compounds (Figure 1f). ^{64}Cu -cyclen was also highly inert toward NO and HNO at a 100 μM concentration (see Figure S4). These results clearly demonstrate that ^{64}Cu -cyclen reacts with H_2S with

high selectivity without any interference from other compounds, even with a maximum 500-fold excess of NaHS. Three other probes, ^{64}Cu -TACN, cyclam, and ATTCD, also showed high selectivity (see Table S2).

We also tested the selectivity of ^{64}Cu -cyclen for H_2S over other polysulfides (see Figure S5). Even though Na_2S_2 , Na_2S_4 , and K_2S_n showed some reactivity with ^{64}Cu -cyclen at a concentration of 12 μM (< 3.4% decomplexation), H_2S showed more than 30-fold higher reactivity with ^{64}Cu -cyclen at the same concentration (100% decomplexation). ^{64}Cu -cyclen, which showed the best results in both the sensitivity and selectivity studies with H_2S , is a small inorganic compound with high water solubility. The octanol-water partition coefficient (LogP) of ^{64}Cu -cyclen was measured to be -3.03 ± 0.03 . Its high sensitivity against H_2S was also maintained in phosphate-buffered saline (PBS), in fetal bovine serum (FBS), and at higher salt concentrations, such as 1M NaCl (see Figure S6a). The protein binding of ^{64}Cu -cyclen was less than 5%. ^{64}Cu -cyclen was stable in PBS at room temperature for up to 28 h (see Figure S7). Copper(II) ions have a very high binding affinity for cyclen ($\log K = 24.8$). The specific activity of ^{64}Cu -cyclen was in the range of 1000–1700 MBq μg^{-1} .

^{64}Cu -cyclen showed a good correlation between decomplexation and H_2S concentration only up to 6 μM (Figure 1e). In contrast, ^{64}Cu -TACN showed excellent linearity over a wider concentration range (see Figure S8a). The decomplexation percentage increased linearly, up to 60 μM H_2S (Figure 1e). For the rapid and reproducible detection of H_2S in biological samples, we tested various TLC conditions and found that the combination of instant TLC (ITLC)^[16] and 2% sodium dodecyl sulfate (SDS) solution as the developing solvent was most effective. Under these conditions, the decomplexed ^{64}CuS remained at the TLC origin, but all intact ^{64}Cu -TACN complexes and any other ^{64}Cu adducts moved with the surfactant SDS solution (see Figure S8b). No interaction between ^{64}CuS and blood components was observed (see Figure S9).

The H_2S concentration in the plasma of Sprague–Dawley (SD) rats was measured by TLC (^{64}Cu -TACN) and the methylene blue (MB) method.^[4] The H_2S concentration in plasma was measured as $(23.8 \pm 7.0) \mu\text{M}$ by using the MB method.^[17] In contrast, the TLC method yielded a much lower concentration, $(2.96 \pm 0.42) \mu\text{M}$, which falls within a range comparable to free H_2S concentrations measured by the monobromobimane/HPLC method.^[18] The large discrepancy between these two methods might arise from the different detection mechanisms employed; whereas ^{64}Cu -TACN reacts only with free H_2S , the MB method detects all sulfide pools in biological samples.^[19] The TLC method has advantages over the MB method, as it is characterized by a simple incubation process, no need for additional chemicals, a short measurement time, and no interference due to the presence of pigments in the sample.^[4]

We then turned to the in vivo detection of H_2S with ^{64}Cu -cyclen. We hypothesized that ^{64}Cu -cyclen could extravascularly circulate through the entire body and react with H_2S to form an insoluble ^{64}CuS precipitate with prolonged retention in lesions. We could then detect radioactive ^{64}CuS by nuclear

imaging. Radioactive ^{64}Cu can also be imaged by luminescence imaging because ^{64}Cu emits relatively strong Cerenkov luminescence during the β -decay process. To test our hypothesis, we administered four different treatments—Matrigel alone or Matrigel mixed with NaCl (1 mg), H_2S solution freshly prepared by bubbling H_2S into water (30 μL), or NaHS (50 μg)—to the back muscle of rats, followed by an immediate injection of ^{64}Cu -cyclen into the tail vein. The animals were then imaged with an optical imager. As expected, Cerenkov luminescence was detected only at the injection sites of the H_2S gas solution and NaHS (Figure 2a). When the same rat was further imaged by using an animal PET scanner at 4 h post-injection, the H_2S and NaHS injection sites could be clearly visualized (Figure 2b). This result clearly indicates that ^{64}Cu -cyclen immediately reacts with H_2S to form ^{64}CuS , and that the formed ^{64}CuS remains in the lesion for a sufficient amount of time to be detected by imaging. The long retention of CuS was further demonstrated by direct inoculation of ^{64}CuS along with free $^{64}\text{CuCl}_2$, ^{64}Cu -cyclen, and ^{64}Cu -cyclam (Figure 2c,d). Whereas the luminescence signals of ^{64}Cu -cyclen and ^{64}Cu -cyclam faded very quickly, within 1 h, ^{64}CuS showed greater than 50 % signal retention even at 4 h (Figure 2d,e).

To evaluate ^{64}Cu -cyclen as an imaging probe for H_2S , an acute inflammation model was developed by injection of the complete Freund's adjuvant (CFA) into the right hind paw of BALB/c mice. CFA stimulates endogenous H_2S formation, which results in an increase in the local concentration.^[20] Three structurally similar ^{64}Cu -labeled complexes (^{64}Cu -

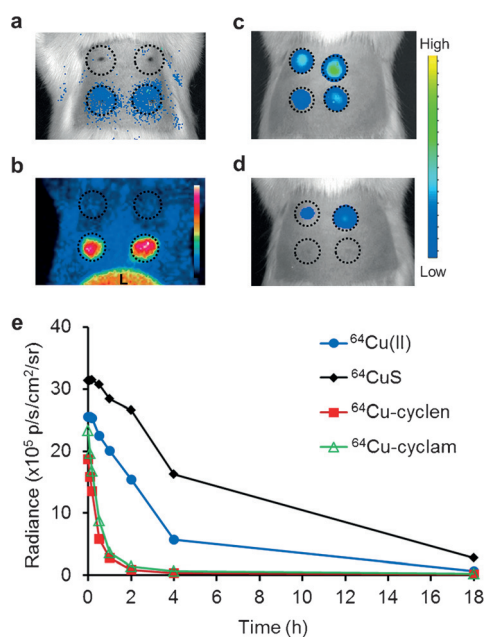


Figure 2. Studies of H_2S detection in animals. a) Cerenkov luminescence images acquired by injecting the back muscle of SD rats with Matrigel alone (top left), Matrigel mixed with NaCl (1 mg; top right), H_2S -gas solution (30 μL ; bottom left), or NaHS (50 μg ; bottom right) at 0 min. b) PET image obtained at 4 h. "L" indicates the liver. c, d) Cerenkov luminescence images acquired by injecting free $^{64}\text{CuCl}_2$ (top left), ^{64}CuS (top right), ^{64}Cu -cyclen (bottom left), and ^{64}Cu -cyclam (bottom right) into the back muscle. The images were taken immediately after injection (c) and at 4 h (d). e) Quantitative analysis of clearance from the injection sites.

cyclen, ^{64}Cu -TACN, ^{64}Cu -cyclam) with different sensitivities for H_2S detection were injected intravenously into these mice. At 1 h post-injection of ^{64}Cu -cyclen, the best signal-to-background ratio was observed at the paw lesion. When the three radiotracers were compared, the highest Cerenkov signal was observed for ^{64}Cu -cyclen, followed by ^{64}Cu -TACN and ^{64}Cu -cyclam (Figure 3a).

The uptake pattern as assessed by PET/CT imaging of the three tracers matched well that of luminescence imaging (Figure 3b). ^{64}Cu -cyclen showed a distinct difference in signal intensity between the inflamed and control paws, whereas ^{64}Cu -cyclam showed only marginal uptake differences. As observed by luminescence imaging, ^{64}Cu -TACN showed an intermediate uptake difference between those of cyclen and cyclam, which reflects the H_2S -detection sensitivity observed in vitro for the three radiotracers (cyclen > TACN > cyclam; Figure 1e). The inflammation/control-paw luminescence signal ratio was quantified as 1.7 ± 0.13 , 1.4 ± 0.05 , and 1.2 ± 0.04 for cyclen, TACN, and cyclam, respectively (see Figure S10a). The PET quantification data also showed similar activity ratios of 2.2 ± 0.22 , 1.7 ± 0.24 , and 1.3 ± 0.11 , respectively. Biodistribution data were in good agreement with the PET imaging data (see Figure S10b). The average H_2S concentration in the inflamed paw was $(7.50 \pm 1.35) \mu\text{M}$, as compared to $(3.07 \pm 0.54) \mu\text{M}$ for the normal paw, on the basis of TLC measurements (Figure 3c). The H_2S concentration ratio (2.4 ± 0.61) between the two paws was in good agreement with the PET signal ratio of ^{64}Cu -cyclen of 2.2 ± 0.22 . These results clearly indicate that our radiotracer maintains sensitivity under physiological conditions, and endogenously generated H_2S can be detected and quantified accurately by both optical and nuclear imaging. Specifically, ^{64}Cu -cyclen showed the highest sensitivity for the detection of H_2S , and PET quantification data reflected the actual H_2S concentration in vivo.

For further confirmation of selective H_2S detection by ^{64}Cu -cyclen under physiological conditions, a H_2S blocking study was performed. DL-Propargylglycine (PPG), an inhibitor of the H_2S -generating enzyme cystathionine- γ -lyase (CSE),^[20] was injected 1 h before CFA injection in the paw inflammation model. After PPG treatment, the uptake in the inflammation paw was dramatically reduced to control levels (Figure 3d). Although the signal decrease was minimal in the control paw,^[21] in the inflamed paw, the percentage of the injected dose per gram (%ID g^{-1}) decreased by 50 %. The inflamed/control-paw uptake ratio decreased from 2.2 ± 0.71 to 1.3 ± 0.25 (Figure 3e). After PPG treatment, the H_2S concentration was also dramatically reduced in the inflamed paw, as observed by PET imaging (Figure 3f).

We performed analogous paw-imaging studies with CSE-knockout (KO, CSE $^{-/-}$) and wild-type (WT, CSE $^{+/+}$) mice^[22] (Figure 3g). Whereas uptake in the control paws of WT and KO mice was comparable, uptake in the inflamed paw in KO mice was significantly lower than that of WT mice. The uptake ratio of the inflamed to the control paw was 2.2 ± 0.42 and 1.6 ± 0.31 in WT and KO mice, respectively (Figure 3h). These data further demonstrate selective H_2S detection by ^{64}Cu -cyclen.

Biodistribution studies were carried out in normal mice to accurately quantify the clearance pattern of the radiotracer (see

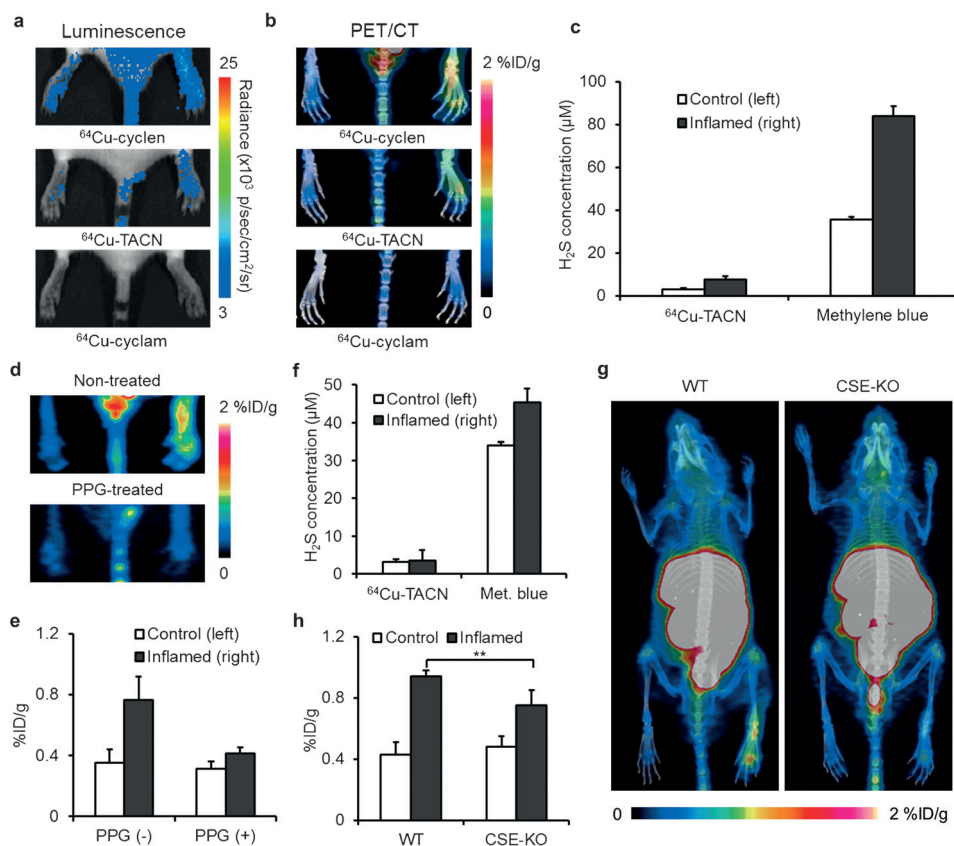


Figure 3. In vivo detection of endogenous H_2S by luminescence and PET imaging in paw inflammation models. a) Cerenkov luminescence images obtained at 1 h. b) PET maximum intensity projection (MIP) images fused with CT images recorded at 1 h. c) H_2S concentration in paw inflammation models ($n=5$). d) Comparative PET-MIP images showing the H_2S -inhibition effect of PPG. e) Quantification analysis based on PET imaging studies ($n=3$). f) Absolute quantification of H_2S in PPG-treated models by using the ^{64}Cu -TACN ($n=7$) and methylene blue methods ($n=5$). g) PET/CT images of ^{64}Cu -cyclen in CSE-KO and WT paw inflammation models. h) Quantification analysis based on PET imaging studies ($n=6$); $^{**}P<0.01$.

Figure S11). Although the injected ^{64}Cu -cyclen cleared rapidly through the kidneys at early time points, more than $25\% \text{ID g}^{-1}$ activity was still observed in the liver and kidneys at 1 h post-injection. These remnant activities, which are thought to be from ^{64}CuS , were then cleared extremely slowly over up to 24 h.

We then moved to an acute myocardial infarction (MI) model.^[23] Recent experimental data strongly suggest that higher H_2S concentrations are induced in infarct lesions to protect against cardiac cell death in MI models.^[24] The detection of an H_2S concentration change in MI models is much more challenging because the heart is located inside the thoracic cavity and an infarct lesion in the heart is only a few millimeters in size. Focal uptake was clearly visualized in the heart region in the transverse section of the fused PET/computed tomography (CT) image (Figure 4a). Two days later, the same rat was injected with 2-deoxy-2- ^{18}F fluoroglucose (^{18}F FDG) and imaged by PET again. A typical donut-shaped myocardium with one portion missing was observed in the transverse image (Figure 4b). Healthy myocardium readily takes up the glucose analogue, ^{18}F FDG, as an energy source; however, the infarct lesion showed markedly reduced uptake.^[25] When two PET images were coregistered with the CT image, the focal hot spot of ^{64}Cu -cyclen perfectly matched the defect site in the donut-

shaped myocardium of the ^{18}F FDG image (Figure 4c). As a negative control, no focal uptake of ^{64}Cu -cyclen was observed in the myocardium of the healthy rat (see Figure S12b). In contrast, when NaHS solution was injected directly into the myocardium before the tail-vein injection of ^{64}Cu -cyclen, the focal uptake of ^{64}Cu -cyclen in the healthy heart was analogous to that observed in MI models (see Figure S12a,c). These results clearly indicate that the high uptake of ^{64}Cu -cyclen in the MI lesion was due to increased H_2S concentrations.

High focal uptake in the infarct lesion was confirmed by an ex vivo autoradiogram (Figure 4d). Triphenyltetrazolium chloride (TTC) staining of the same heart section showed a white infarct lesion, which was well-matched with the high-activity lesion of the autoradiogram (Figure 4e). The adjacent heart slice was further investigated by Masson's trichrome staining (Figure 4f). Upon quantification, the uptake of ^{18}F FDG was 2.5-fold (± 0.76) greater in the healthy lesion, whereas that of ^{64}Cu -cyclen was 4.5-fold (\pm

1.18) higher in the infarct lesion (Figure 4h). This result indicates that the infarct lesion could be more readily detected by ^{64}Cu -cyclen. ^{64}Cu -cyclen imaging is also advantageous in that positive uptake is measured rather than negative uptake as with ^{18}F FDG. For ex vivo confirmation, the infarcted heart was cut into six pieces, and activity was counted by using a gamma counter. The piece containing most of the infarct lesion (#1) showed approximately fourfold higher uptake as compared to the other heart pieces (Figure 4i), in analogy with the PET quantification data. The H_2S concentration in the infarct lesion (#1) was measured as $(11.4 \pm 1.6) \mu\text{M}$, whereas the H_2S concentration in section 6 was $(3.52 \pm 1.13) \mu\text{M}$. The other four areas showed intermediate concentrations, which is generally consistent with the activity uptake pattern in biodistribution studies (Figure 4i). Together, these data clearly demonstrate that elevated H_2S concentrations, in infarction lesions of only a few millimeters in size, could be imaged with good spatial resolution by PET imaging, and could be quantified without an invasive biopsy. Neither Cu-cyclen (see Figure S13) nor CuS (see Figure S14) showed any noticeable cytotoxicity in an MTT assay.

In summary, we have developed new chemical tools for the detection, quantification, and in vivo imaging of endog-

enous H_2S in live animals. ^{64}Cu -cyclen showed a sub-micromolar detection limit and high selectivity for H_2S over other potential competitors, including polysulfides. The H_2S concentration in biological samples was instantly measured without harsh sample pretreatment. The increased endogenous H_2S concentration was clearly imaged and quantified by a human-applicable nuclear imaging technique in two different disease models. Overall, by the use of a new gas-trapping strategy, many obstacles of previous methods were overcome. Our methods could be efficiently used in H_2S biology and medicine.

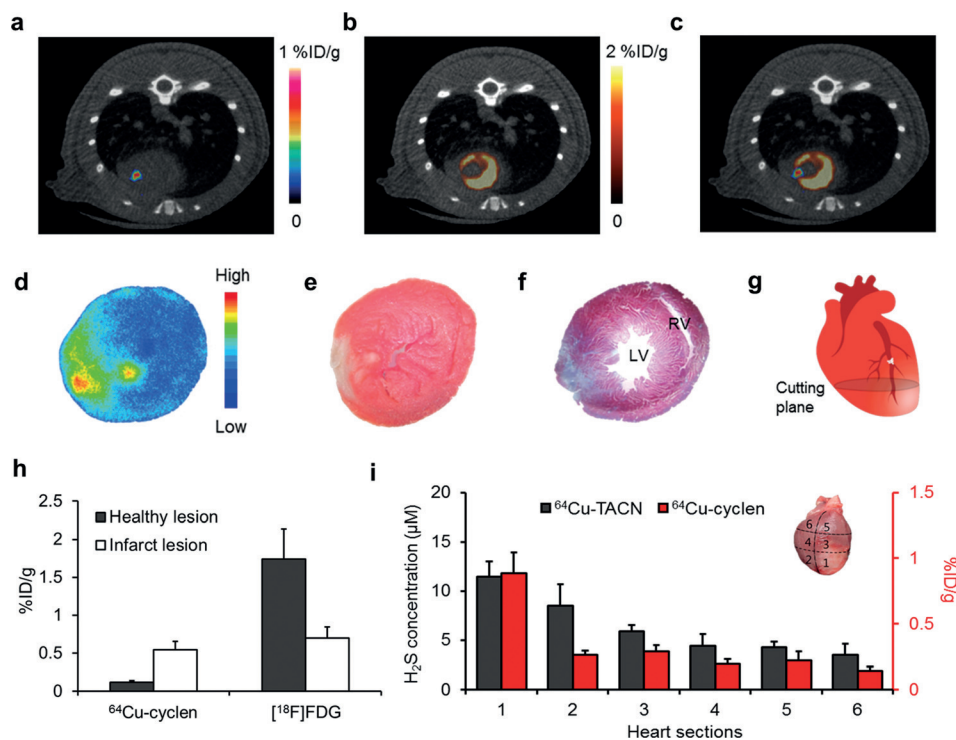


Figure 4. PET/CT imaging in MI models and ex vivo validation of the excised MI heart. a) Transverse PET/CT image of the MI model at 4 h with ^{64}Cu -cyclen. b) Transverse PET/CT image of the same MI model at 1 h with $[^{18}\text{F}]\text{FDG}$. c) Coregistered fusion image of ^{64}Cu -cyclen and $[^{18}\text{F}]\text{FDG}$. d) Ex vivo autoradiogram, e) TTC staining, and f) Masson's trichrome staining of the excised heart of an MI model at 4 h with ^{64}Cu -cyclen. LV, left ventricle; RV, right ventricle. g) Schematic drawing showing the cutting plane of the MI heart. The infarct lesion is marked by a white blur. h) Quantification analysis in PET imaging ($n=4$ each). i) H_2S concentrations measured with ^{64}Cu -TACN in MI hearts ($n=5$). Biodistribution data are displayed in red ($n=3$). A heart was cut into six pieces as shown inside the graph.

Acknowledgements

This research was supported by the R&D Program of the National Research Foundation of Korea, which is funded by the Ministry of Science, ICT and Future Planning (No. 2013M2A2A6042317, 20120006386, 2013R1A4A1069507). The Korea Basic Science Institute (Daegu) is acknowledged for providing assistance with the NMR and MS measurements.

Keywords: gas immobilization · hydrogen sulfide · imaging agents · nuclear imaging · radioisotopes

How to cite: *Angew. Chem. Int. Ed.* **2016**, *55*, 9365–9370
Angew. Chem. **2016**, *128*, 9511–9516

- [1] C. Szabo, *Nat. Rev. Drug Discovery* **2007**, *6*, 917–935.
- [2] D. J. Polhemus, D. J. Lefer, *Circ. Res.* **2014**, *114*, 730–737.
- [3] Y. Takano, K. Shimamoto, K. Hanaoka, *J. Clin. Biochem. Nutr.* **2016**, *58*, 7–15.
- [4] P. Nagy, Z. Pálkás, A. Nagy, B. Budai, I. Tóth, A. Vasas, *Biochim. Biophys. Acta Gen. Subj.* **2014**, *1840*, 876–891.
- [5] N. S. Lawrence, J. Davis, R. G. Compton, *Talanta* **2000**, *52*, 771–784.
- [6] N. Kumar, V. Bhalla, M. Kumar, *Coord. Chem. Rev.* **2013**, *257*, 2335–2347.
- [7] A. R. Lippert, E. J. New, C. J. Chang, *J. Am. Chem. Soc.* **2011**, *133*, 10078–10080.
- [8] K. Sasakura, K. Hanaoka, N. Shibuya, Y. Mikami, Y. Kimura, T. Komatsu, T. Ueno, T. Terai, H. Kimura, T. Nagano, *J. Am. Chem. Soc.* **2011**, *133*, 18003–18005.
- [9] Y. Chen, C. Zhu, Z. Yang, J. Chen, Y. He, Y. Jiao, W. He, L. Qiu, J. Cen, Z. Guo, *Angew. Chem. Int. Ed.* **2013**, *52*, 1688–1691; *Angew. Chem.* **2013**, *125*, 1732–1735.
- [10] R. Weissleder, M. J. Pittet, *Nature* **2008**, *452*, 580–589.
- [11] X. J. Zou, Y. C. Ma, L. E. Guo, W. X. Liu, M. J. Liu, C. G. Zou, Y. Zhou, J. F. Zhang, *Chem. Commun.* **2014**, *50*, 13833–13836.
- [12] M. D. Hammers, M. J. Taormina, M. M. Cerda, L. A. Montoya, D. T. Seidenkranz, R. Parthasarathy, M. D. Pluth, *J. Am. Chem. Soc.* **2015**, *137*, 10216–10223.
- [13] J. Cao, R. Lopez, J. M. Thacker, J. Y. Moon, C. Jiang, S. N. S. Morris, J. H. Bauer, P. Tao, R. Mason, A. Lippert, *Chem. Sci.* **2015**, *6*, 1979–1985.
- [14] M. Rudin, *Curr. Opin. Chem. Biol.* **2009**, *13*, 360–371.
- [15] J. R. Goates, M. B. Gordon, N. D. Faux, *J. Am. Chem. Soc.* **1952**, *74*, 835–836.
- [16] K. Itiaba, J. Crawhall, C. Sin, *Clin. Biochem.* **1970**, *3*, 287–293.
- [17] X. Zhou, Y. Feng, Z. Zhan, J. Chen, *J. Biol. Chem.* **2014**, *289*, 28827–28834.
- [18] H. Yang, Y. Mao, B. Tan, S. Luo, Y. Zhu, *Eur. J. Pharmacol.* **2015**, *761*, 135–143.
- [19] A. Papapetropoulos, M. Whiteman, G. Cirino, *Br. J. Pharmacol.* **2015**, *172*, 1633–1637.
- [20] L. Li, M. Bhatia, Y. Z. Zhu, Y. C. Zhu, R. D. Ramnath, Z. J. Wang, F. B. Anuar, M. Whiteman, M. Salto-Tellez, P. K. Moore, *FASEB J.* **2005**, *19*, 1196–1198.
- [21] H. Zhang, S. M. Mochhala, M. Bhatia, *J. Immunol.* **2008**, *181*, 4320–4331.
- [22] I. Ishii, N. Akahoshi, H. Yamada, S. Nakano, T. Izumi, M. Suematsu, *J. Biol. Chem.* **2010**, *285*, 26358–26368.
- [23] T. N. Johns, B. J. Olson, *Ann. Surg.* **1954**, *140*, 675–682.
- [24] A. Sivarajah, M. McDonald, C. Thiernemann, *Shock* **2006**, *26*, 154–161.
- [25] W. W. Lee et al. *J. Am. Coll. Cardiol.* **2012**, *59*, 153–163.

Received: April 20, 2016

Revised: June 5, 2016

Published online: July 8, 2016